

Stronger super typhoons in a warmer world

N-Y Kang^{1,2} and J B Elsner¹

Florida State University, Tallahassee, FL 32306, USA

Korea Meteorological Administration, Seoul 156720, South Korea

E-mail: nkang@fsu.edu

1. Introduction

The changing nature of tropical cyclone (TC) climate is an important concern in relation to anthropogenic global warming. Past studies are limited to separate analysis of observables such as frequency and intensity [3, 9, 10, 6, 7, 2]. Here those observables in tandem provide orthogonal axes for an integrated framework that allows us to project global sea-surface temperature (SST) and El Niño variations onto a complete range of TC climate in the western North Pacific, the most prolific of the TC regions accounting for over a third of all TCs worldwide.

We organize a set of TC best-tracks from the Joint Typhoon Warning Center (JTWC, www.usno.navy.mil/NOOC/nmfc-ph/RSS/jtwc/best_tracks) and the Japan Meteorological Agency (JMA, www.jma.go.jp/jma/jma-eng/jma-center/rsmc-hp-pub-eg). The former uses one-minute average convention for wind speed, while the latter ten-minute average convention. Annual frequency and intensity variations in the western North Pacific are made into each single variation using principal component eigenvector from the two best-tracks. The eigenvector is the joint independent addition of JMA and JTWC variations.

To investigate the environmental relationships with TC climate, Southern Oscillation Index (SOI) and SST data are used. SOI index comes from the NOAA Earth System Research Laboratory (ESRL, www.esrl.noaa.gov/psd/data/climateindices). Annual values of negative SOI are used for El Niño variation. For SST we utilize monthly SSTs from the National Oceanic and Atmospheric Administration (NOAA) Extended Reconstructed Sea Surface Temperature (ERSST) V3b (www.esrl.noaa.gov/psd/data/gridded).

We find that the orientation of the highest correlation with rising global SST projects significantly onto the axes defined as the efficiency of intensity consistent with fewer but stronger TCs. Computations are made for the TC season that runs from June to November and extends over the 28-year(1984–2011) period [5]. All statistics and figures are created using the software R (www.r-project.org) and are available from rpubs.com/Namyong/D201301.

2. Framework for TC climate analysis

Figure 1 illustrates the empirical framework and shows the relationship between western North Pacific TC climate and both global warming and El Niño. The annual variation in TC frequency, obtained by counting cyclones whose lifetime maximum wind speed (LMW) exceeds 17 m s^{-1} , is placed on the axis denoted as FRQ. The annual intensity variation of these TCs, obtained by averaging the LMW for the same set of cyclones and denoted INT, is placed on an axis orthogonal to FRQ.

A principal component eigenvector indicating the joint independent addition of INT and FRQ is defined as activity (ACT). This definition of ACT is similar to accumulated cyclone energy [1]. Importantly, the framework introduces a new TC indicator that is orthogonal to ACT, that we term the efficiency of intensity (EINT), that captures the intensity contribution of ACT [4]. More generally the framework provides a novel TC climate indicator (TCI_θ) computed as

$$\text{TCI}_\theta = \text{INT} \cdot \cos \theta + \text{FRQ} \cdot \sin \theta, \quad (1)$$

where θ is the direction angle away from INT (positive is counterclockwise). The variables INT and FRQ are scaled to be centered on zero with unit variance. Since correlation is a quantity without units, we create a correlation screen that compares the influence of environmental factors using all TCI directions.

The light blue circle maps the correlation between El Niño and TC climate on the correlation screen. Among the range of significant ($\alpha \leq 0.05$) correlation (dark blue line), the highest value ($r = +.77$ [.55, .89] 95% CI) appears in the direction of ACT (dark blue dot). This distinguishes ACT as more sensitive to El Niño than either FRQ or INT alone. In comparison, the orange circle maps the correlation between TC climate and global SST. The significant correlation range (red line) and the highest correlation ($r = +.70$ [.44, .85] 95% CI) appear in the direction of EINT (red dot).

EINT is the out-of-phase relationship between TC frequency and intensity. The out-of-phase relationship is strongly linked with global SST, while the in-phase relationship with El Niño. The empirical framework shows global SST has an influence on TC climate that is orthogonal to El Niño's influence. It also clearly shows why attempts to link SST with observed TC frequency and intensity have not been successful. By regarding ACT as TC energy, the influence of global SST on TC climate is a regulator of this energy that is interpreted as the efficiency of intensity.

3. Typhoon climate aspect at higher intensity levels

Figure 2 summarizes results of applying the framework and computing correlations for TCs at increasing intensity levels. For example, here 30% of the strongest TCs correspond to LMW that exceed the 0.7 quantile threshold. The INT axis is calculated by averaging the LMWs for TCs that exceed this threshold each year. The FRQ axis uses all TCs to limit distortions arising from small counts at the highest intensity levels.

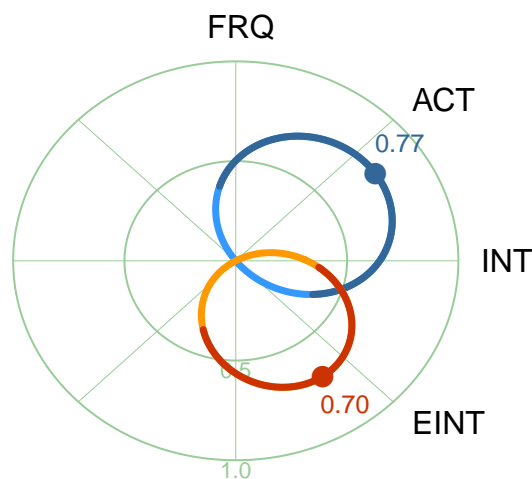


Figure 1. Correlation screen of TC climate indicators. Center, inner circle and outer circle indicate the correlation levels of 0, 0.5 and 1, respectively. Light blue and orange lines show the correlation values of El Niño and global SST for every direction of western North Pacific TC climate during the TC season (June–November) over 28 years (1984–2011). Dark blue and red lines represent the significant ($\alpha \leq 0.05$) range of correlations. Dots indicate the direction of largest correlation.

The three panels represent the correlations with El Niño, global SST and the joint independent addition of El Niño and global SST, respectively. Correlation values are calculated at 22.5° and 10% intervals and placed on the horizontal and vertical axes, respectively. Significant correlations ($\alpha \leq 0.05$) are shown as colored dots. Every intensity level shows the same structure as in figure 1. The highest correlations with El Niño (transparent blue line) appear in the direction of ACT, while the highest correlations with global SST (transparent red line) appear in the direction of EINT. Correlations with the joint independent addition of El Niño and global SST (transparent purple line) align along the INT axis between ACT and EINT confirming their orthogonal roles in influencing TC climate.

We also find significant and strong correlations between global SST and intensity efficiency at higher TC intensity (figure 2(b)). We note that the joint independent addition of El Niño and global SST explains well the INT at all intensity levels (figure 2(c)). Since El Niño and global SST are highly correlated respectively with ACT and EINT, this reversed principal component eigenvector results in strong correlation with INT and confirming the fact that neither El Niño or global SST alone can successfully explain TC intensity variation.

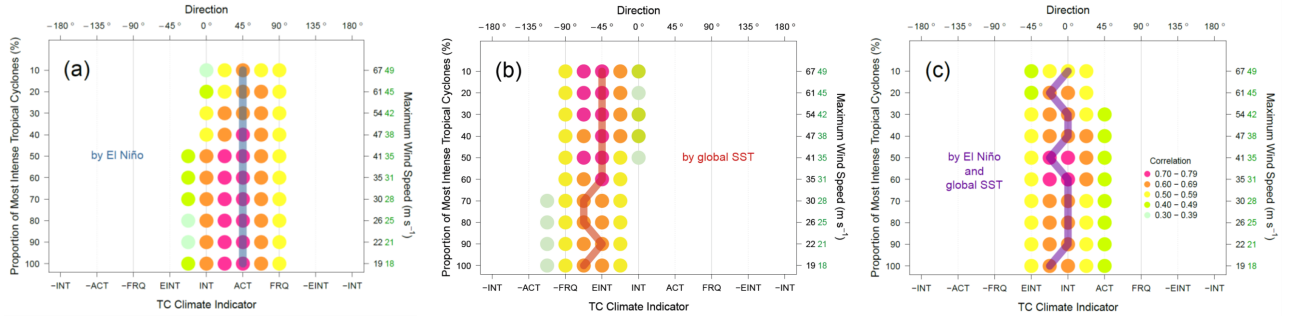


Figure 2. The highest correlation as a function of direction and proportion of most intense TCs. Correlation coefficients with **a** El Niño, **b** global SST and **c** principal component eigenvector that describes the joint independent addition of El Niño and global SST. Global TC climate, SOI and SST during the TC season (June–November) over 28 years (1984–2011) are used for the plots. The values are calculated at 22.5° and 10% intervals for the horizontal and vertical axes, respectively. Transparent blue, red and purple lines are linking the directions of the highest correlation among TC climate indicators. Only significant ($\alpha \leq 0.05$) correlations are shown in circles filled with colors. The average of threshold wind speeds at intensity levels are shown on the right axis. Black and green characters represent the wind speeds from JTWC and JMA, respectively.

4. Influence of global warming on super typhoons

Figure 3 compares annual variation in global SST (red line) with annual variation in TC climate (green line) at $\theta = -45^\circ$ (the EINT axis) and for the upper 10% of the strongest TCs in the western North Pacific (see figure 3(b)). The averaged threshold wind speeds for this subset are 67 m s^{-1} in JTWC, which nearly matches the super typhoons of category 5 on the Saffir-Simpson scale [8]. Trends and annual fluctuations over the 28-year (1984–2011) period confirm a tight connection between global SST and the efficiency of TC intensity. The SST trend over the period is $+2.9 \pm 0.43 \text{ s.d./30 yr}$ (s.e.) which compares with the trend in the intensity efficiency of $+2.1 \pm 0.56 \text{ s.d./30 yr}$ (s.e.). The correlation between the two series is $+0.73$ [0.49, 0.87] 95% CI that reduces to $+0.52$ [0.18, 0.75] 95% CI after removing the linear trends.

The efficiency of typhoon intensity in figure 3 is understood as the intensity variation at the same level of TC energy. Once a large amount of TC energy is given by El Niño, stronger super typhoons are possible with higher global SST conditions. El Niño events may seem to increase the typhoon extremes with time, but it is global warming that works to increase the efficiency of typhoon intensity.

5. Summary

A novel empirical framework for tropical cyclone climate is used to shed broader light on the societally-relevant relationship between typhoons and global warming. The

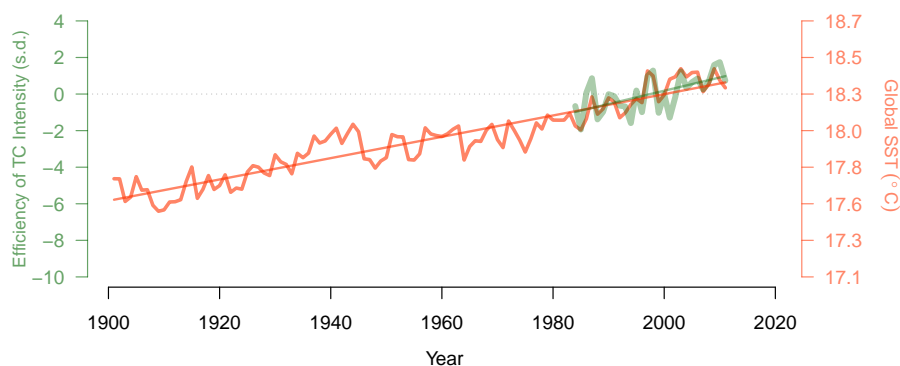


Figure 3. Time series of global SST (red line) and efficiency of TC intensity (green line). The efficiency of TC intensity is computed using $\theta = -45^\circ$ and 10% of most intense TCs (see figure 2(b)). Values are standardized to the 28-year (1984–2011) period and the scale for the SST values are presented on the right axis. The 111-year global SST trend and the 28-year TC climate trend are shown as red and green straight lines.

warming seas are providing additional energy to produce more extreme TCs [2] but this is happening at the expense of typhoon frequency in the western North Pacific. The results imply that record-breaking typhoon intensities are likely under global warming regardless of the increase of TC energy.

Acknowledgements

This research was supported by Geophysical Fluid Dynamics Institute at Florida State University.

References

- [1] Bell G D *et al.* 2000 *Bull. Am. Meteorol. Soc.* **81** 1328
- [2] Elsner J B, Kossin J P, Jagger T H 2008 *Nature* **455** 92
- [3] Emanuel K E 2005 *Nature* **436** 686
- [4] Kang N-Y, Elsner J B 2012 *Clim. Dyn.* **39** 669
- [5] Kang N-Y, Elsner J B 2012 *J. Clim.* **25** 7564
- [6] Klotzbach P J 2006 *Geophys. Res. Lett.* **33** L10805
- [7] Landsea C W, Harper B A, Hoarau K, Knaff J A 2006 *Science* **313** 452
- [8] Simpson R H 1974 *Weatherwise* **27** 169
- [9] Trenberth K 2005 *Science* **308** 1753
- [10] Webster P J, Holland G J, Curry J A, Chang H-R 2005 *Science* **309** 1844